A 3D semi implicit method for computing the current density in bulk superconductors

A. Kameni[1], M. Boubekeur[1], L. Alloui[1], F. Bouillault[1], J. Lambretchs[2], C. Geuzaine[3]

[1] Laboratoire de Génie Electrique de Paris, UMR 8507 CNRS, Supelec, Université Paris Sud, Université Pierre et Marie Curie, Plateau du Moulon, 91192 Gif-Sur-Yvette Cedex, France

[2] Centre for Systems Engineering and Applied Mechanics, Louvain-la-Neuve, Belgium

[3] University of Liège, Dept of Electrical Engineering and Computer Science, Liège 4000, Belgium

A semi-implicit approach is proposed for computing the current density in superconductors characterized by non linear vectorial power law. A nodal Discontinuous Galerkin method is adopted for the spatial discretization of the non linear system satisfied by the components of the electric field. Explicit developments are used to construct boundary conditions to avoid the modeling of a volume around the superconducting sample. A modified Newton iterative method is introduced for solving the discrete system. Numerical examples on a 2D superconducting plate and a 3D superconducting cube are computed. Distributions of a component of the current density are presented and differences in the diffusive process are highlighted. The penetration time and losses are compared to those obtained with an $A-V$ formulation solved by a Finite Volume method.

***Index Terms*—High temperature superconductors, Maxwell's equations, Discontinuous Galerkin Method, Finite Element Method, Newton iterative method, Semi-implicit approach.**

I. Introduction

Superconducting materials are increasingly introduced in electrical engineering and development of efficient numerical tools is a crucial issue for their characterization. Linear models based on critical state suggested by Bean have been widely used to evaluate losses and magnetization of low temperature superconductors [1], but they are not suitable for high temperature superconductors. Indeed, numerical simulations are notoriously difficult to carry out when a power law description of their behavior is assumed by $J-E$ or $E-J$ relations given by:

$$\frac{\overrightarrow{E}}{E_c} = \left\| \frac{\overrightarrow{J}}{J_c} \right\|^{n-1} \frac{\overrightarrow{J}}{J_c} \tag{1}$$

$$\frac{\overrightarrow{J}}{J_c} = \left\| \frac{\overrightarrow{E}}{E_c} \right\|^{\frac{1}{n}-1} \frac{\overrightarrow{E}}{E_c} \tag{2}$$

with, $\overrightarrow{J}$ the current density, $\overrightarrow{E}$ the electric field, E_c the critical electric field, J_c the critical current density and the exponent $n > 1$ that characterizes the flux creep phenomena [2] ($n = 1$ corresponds to a normal conductor and $n = +\infty$ coincides with the Bean critical state).

Different discretization techniques have been implemented for computing 2D induced fields in superconducting materials [3] [4]. For the 3D case, the classical finite element method (FEM) is often used to deal with the $E-J$ power law [6] [7]. Discretization concerns spatial operators with a nonlinear term of type $\overrightarrow{\nabla} \times \overrightarrow{\nabla} \left(\left\| \frac{\overrightarrow{J}}{J_c} \right\|^{n-1} \frac{\overrightarrow{J}}{J_c} \right)$ or $\overrightarrow{\nabla} \cdot \overrightarrow{\nabla} \left(\left\| \frac{\overrightarrow{J}}{J_c} \right\|^{n-1} \frac{\overrightarrow{J}}{J_c} \right)$. Unfortunately, during computation of the discrete solution spurious oscillations often appear. In addition, a surrounding vacuum volume is added to set the boundary conditions. This leads to solving additional equations and increases the computational cost.

In this paper, the $J-E$ form (2) of the constitutive law is considered and the differential system satisfied by the electric field is defined. The spatial operator is kept linear and the nonlinearity is then carried by the temporal term. Our work is based on the discretization of the scalar Laplacian operator using a nodal discontinuous Galerkin method. The interface flux terms are obtained from the symetric interior penality method [8]. A semi-implicit scheme that consists in solving the three non linear diffusion equations satisfied by the components of the electric field is proposed. The boundary conditions are defined thanks to explicit developments of Maxwell-Gauss and Maxwell-Faraday relations to avoid using a surounding volume. They take into account the demagnetizing field created by the sample. This work is an extension of the method published previously to compute vectorial 2D current density distributions in superconductors [9].

II. The differential system

In a three-dimensional setting where the magnetic induction is $\overrightarrow{B} = (B_x, B_y, B_z)$, the electric field and the current density have three nonzero components. They satisfy a vectorial problem written as:

$$\mu_0 \frac{\partial \overrightarrow{J}}{\partial t} - \overrightarrow{\triangle} \overrightarrow{E} = -\overrightarrow{\nabla} \overrightarrow{\nabla} \cdot \overrightarrow{E} \tag{3}$$

The main idea of this article is to solve the diffusion equations of each component with an explicit coupling. We set $u_1 = E_x/E_c$, $u_2 = E_y/E_c$, $u_3 = E_z/E_c$, $v_1 = J_x/J_c$, $v_2 = J_y/J_c$, $v_3 = J_z/J_c$, $c = \mu_0 J_c/E_c$ and $(S_1, S_2, S_3) = -\overrightarrow{\nabla} \overrightarrow{\nabla} \cdot \left(\overrightarrow{E}/E_c \right)$ and define the following functions to take into account the $3D$ behavior:

$$\beta_1(u_1,u_2,u_3)=\left(u_1^2+u_2^2+u_3^2\right)^{\frac{1-n}{2n}}u_1=v_1 \tag{4}$$

$$\beta_2(u_1,u_2,u_3)=\left(u_1^2+u_2^2+u_3^2\right)^{\frac{1-n}{2n}}u_2=v_2 \tag{5}$$

$$\beta_3(u_1,u_2,u_3)=\left(u_1^2+u_2^2+u_3^2\right)^{\frac{1-n}{2n}}u_3=v_3 \tag{6}$$

such that $\beta_1(0,u_2,u_3)=0$, $\beta_2(u_1,0,u_3)=0$ and $\beta_3(u_1,u_2,0)=0$.

The system of three non linear diffusion equations is completed by fluxes boundary conditions, leading to the following system :

$$(S)\left\{\begin{array}{l}\dfrac{\partial\beta_1(u_1,u_2,u_3)}{\partial t}-c^{-1}\triangle u_1=S_1 \text{ in } \Omega\\ \dfrac{\partial\beta_2(u_1,u_2,u_3)}{\partial t}-c^{-1}\triangle u_2=S_2 \text{ in } \Omega\\ \dfrac{\partial\beta_3(u_1,u_2,u_3)}{\partial t}-c^{-1}\triangle u_3=S_3 \text{ in } \Omega\\ \overrightarrow{\nabla}u_1\cdot\overrightarrow{\nu}=C_{b_1}(t) \text{ on } \partial\Omega\\ \overrightarrow{\nabla}u_2\cdot\overrightarrow{\nu}=C_{b_2}(t) \text{ on } \partial\Omega\\ \overrightarrow{\nabla}u_3\cdot\overrightarrow{\nu}=C_{b_3}(t) \text{ on } \partial\Omega\end{array}\right. . \tag{7}$$

where $C_{b_{1,2,3}}$ are built from Faraday's law and the assumption that $\overrightarrow{\nabla}\cdot\overrightarrow{E}=0$ holds outside the sample.

Existence and unicity of solutions are ensured since $\beta_{1,2,3}$ are monotoneous lipschitzian functions. The proof is obtained from the study of quasy linear elliptic and parabolic equations [10].

III. Semi-implicit approach and discrete system

A. *Semi-implicit coupling approach*

The semi implicit coupling approach consist in using the previous solutions u_2^k, u_3^k at time $t=t_k$ for computing the solution u_1^{k+1} at time $t=t_{k+1}$ (similarly for u_2^{k+1} and u_3^{k+1}).

We note $\beta_1(u_1^{k+1})=\beta_1(u_1^{k+1},u_2^k,u_3^k)$, $\beta_2(u_2^{k+1})=\beta_2(u_1^k,u_2^{k+1},u_3^k)$ and $\beta_3(u_3^{k+1})=\beta_3(u_1^k,u_2^k,u_3^{k+1})$. Our coupling approach leads to these expressions of nonlinearities:

$$\beta_1(u_1^{k+1})=\left[\left(u_1^{k+1}\right)^2+\left(u_2^k\right)^2+\left(u_3^k\right)^2\right]^{\frac{1-n}{2n}}u_1^{k+1} \tag{8}$$

$$\beta_2(u_2^{k+1})=\left[\left(u_1^k\right)^2+\left(u_2^{k+1}\right)^2+\left(u_3^k\right)^2\right]^{\frac{1-n}{2n}}u_2^{k+1} \tag{9}$$

$$\beta_3(u_3^{k+1})=\left[\left(u_1^k\right)^2+\left(u_2^k\right)^2+\left(u_3^{k+1}\right)^2\right]^{\frac{1-n}{2n}}u_3^{k+1} \tag{10}$$

B. *Boundary conditions*

The main difficulty in superconductor modeling is to taking into account the demagnetizing effects. It is common to add a volume around the sample to set boundary conditions at its borders [11], but this result in increasing the computational cost. Equivalent flux boundary conditions based on computing $\overrightarrow{\nabla}u_{1,2,3}$ are proposed to avoid this technique. Their components are expressed thanks to explicit developments of $\overrightarrow{\nabla}\cdot\overrightarrow{E}=0$ and $\overrightarrow{\nabla}\times\overrightarrow{E}=-\dfrac{\partial\overrightarrow{B}}{\partial t}$ on $\partial\Omega$. These developments result in:

$$\left\{\begin{array}{l}\dfrac{\partial u_1^{k+1}}{\partial x}=-\dfrac{\partial u_2^k}{\partial y}-\dfrac{\partial u_3^k}{\partial z}\\ \dfrac{\partial u_1^{k+1}}{\partial y}=\dfrac{\partial u_2^k}{\partial x}+E_c^{-1}\dfrac{\partial B_z}{\partial t}\\ \dfrac{\partial u_1^{k+1}}{\partial z}=\dfrac{\partial u_3^k}{\partial x}-E_c^{-1}\dfrac{\partial B_y}{\partial t}\end{array}\right. \tag{11}$$

$$\left\{\begin{array}{l}\dfrac{\partial u_2^{k+1}}{\partial x}=\dfrac{\partial u_1^k}{\partial y}-E_c^{-1}\dfrac{\partial B_z}{\partial t}\\ \dfrac{\partial u_2^{k+1}}{\partial y}=-\dfrac{\partial u_1^k}{\partial x}-\dfrac{\partial u_3^k}{\partial z}\\ \dfrac{\partial u_3^{k+1}}{\partial z}=\dfrac{\partial u_3^k}{\partial y}+E_c^{-1}\dfrac{\partial B_x}{\partial t}\end{array}\right. \tag{12}$$

$$\left\{\begin{array}{l}\dfrac{\partial u_3^{k+1}}{\partial x}=\dfrac{\partial u_1^k}{\partial z}+E_c^{-1}\dfrac{\partial B_y}{\partial t}\\ \dfrac{\partial u_3^{k+1}}{\partial y}=\dfrac{\partial u_2^k}{\partial z}-E_c^{-1}\dfrac{\partial B_x}{\partial t}\\ \dfrac{\partial u_3^{k+1}}{\partial z}=-\dfrac{\partial u_1^k}{\partial x}-\dfrac{\partial u_2^k}{\partial y}\end{array}\right. \tag{13}$$

At $t=t_{k+1}$, the total magnetic field is defined as: $\overrightarrow{B}=\overrightarrow{B_a}+\overrightarrow{B_d}$, with $\overrightarrow{B_a}$ the uniform applied magnetic field at $t=t_{k+1}$ and $\overrightarrow{B_d}$ the demagnetized field created by the sample computed at t_k. The quasi-static approximation of electromagnetic fields defines the average demagnetizing field as: $\overrightarrow{B}_d=-\mu_0\bar{\bar{N}}\overrightarrow{M}$, where $\bar{\bar{N}}$ is a tensor of the demagnetizing factors and M is the magnetization given at $t=t_k$ by: $\overrightarrow{M^k}=0.5V\int_V\overrightarrow{r}\times\overrightarrow{J^k}dV$, with $\overrightarrow{r}=(x,y,z)$ and V the volume of the sample. For the most common geometries $\bar{\bar{N}}$ is computed from analytical formulas [12].

C. *The discrete system*

Spatial discretization of the Laplacian operator in system (7) is performed. The generated terms and the boundary conditions are represented by $F_{1,2,3}$. The non linear algebric system is given by: matrix M_{DG}:

$$\left\{\begin{array}{l}M_{DG}\dfrac{\beta_1(u_1^{k+1})-\beta_1(u_1^k)}{\delta t}=F_1(u_1^{k+1},u_2^k,u_3^k)\\ M_{DG}\dfrac{\beta_2(u_2^{k+1})-\beta_2(u_2^k)}{\delta t}=F_2(u_1^k,u_2^{k+1},u_3^k)\\ M_{DG}\dfrac{\beta_3(u_3^{k+1})-\beta_3(u_3^k)}{\delta t}=F_3(u_1^k,u_2^k,u_3^{k+1})\end{array}\right. \tag{14}$$

where M_{DG} is the global mass matrix. To avoid difficulties in linearization - that introduces the fact that β_1, β_2 and β_3 are not continuous derivables at 0 - a changing of discrete unknowns is proposed. The components of current density v_1, v_2, v_3 are choosen as the new unknowns. They are computed from an equivalent algebric system given by:

$$\left\{\begin{array}{l}M_{DG}\dfrac{v_1^{k+1}-v_1^k}{\delta t}=G_1(v_1^{k+1},v_2^k,v_3^k)\\ M_{DG}\dfrac{v_2^{k+1}-v_2^k}{\delta t}=G_2(v_1^k,v_2^{k+1},v_3^k)\\ M_{DG}\dfrac{v_3^{k+1}-v_3^k}{\delta t}=G_3(v_1^k,v_2^k,v_3^{k+1})\end{array}\right. \tag{15}$$

where $G(v_1,v_2,v_3)=F(u_1,u_2,u_3)$.

The linearization of G is ensured if the inverse functions β_1^{-1} β_2^{-1} β_3^{-1} exist and are derivables. Unfortunately, these derivatives are non trivial. In accordance with the $E-J$ power law (1), we suppose that :

$$u_1^{k+1} = \beta_1^{-1}(v_1^{k+1}) = \left[\left(v_1^{k+1}\right)^2 + \left(v_2^{k}\right)^2 + \left(v_3^{k}\right)^2\right]^{\frac{n-1}{2}} v_1^{k+1} \quad (16)$$

$$u_2^{k+1} = \beta_2^{-1}(v_2^{k+1}) = \left[\left(v_1^{k}\right)^2 + \left(v_2^{k+1}\right)^2 + \left(v_3^{k}\right)^2\right]^{\frac{n-1}{2}} v_2^{k+1} \quad (17)$$

$$u_3^{k+1} = \beta_3^{-1}(v_3^{k+1}) = \left[\left(v_1^{k}\right)^2 + \left(v_2^{k}\right)^2 + \left(v_3^{k+1}\right)^2\right]^{\frac{n-1}{2}} v_3^{k+1} \quad (18)$$

These inverse functions are continuous and derivable and a Newton iterative method is applied for computing v_1^{k+1}, v_2^{k+1} and v_3^{k+1} (see [9]). The time step of the numerical scheme has the same order as that is given by the CFL condition of the linear diffusion equation with $n = 1$.

IV. Numerical results

We consider a superconductor sample of characteristics: $J_c = 500A/mm^2$, $E_c = 10^{-7}V/mm$ and $n = 13$. It is subjected to an external magnetic field in the z direction: $B_a(t) = a_B t$, with $a_B = 50T/s$. A fast ramping is considered to show robustness of this approach. The Newton iterative method needed less than 5 iterations at each time step δt.

Three configurations are studied:

- A 2D superconducting plate of edge length $a = 2mm$. The mesh has 11700 nodes, $\delta t = 25\mu_s$. The computation time is $1h$ on 1 core.
- A 3D superconducting cube of edge length $a = 2mm$, whose demagnetizing factors are $N_x = N_y = N_z = 1/3$. The mesh has 80000 nodes, $\delta t = 10\mu_s$. The computation time is $3h$ on 10 cores.
- The same 3D superconducting cube with a surrounding cube of edge length $4a/3$ and characteristics $c = \mu_0 J_c/E_c = 0.5$, $n = 1$. The mesh has 170000 nodes, $\delta t = 10\mu_s$. The computation time is $18h$ on the same 10 cores machine. The magnetic field is imposed at border of the surounding volume through flux expresssions previously described. This results in a time shift of the penetration.

The components J_x/J_c and J_y/J_c have the expected symetries due to similarities of their boundary conditions. Iso-value distributions of J_y/J_c are presented in the following figures to describe partial and full penetration. They show $2D-3D$ differences in diffusive process.

Partial penetration: Figs. 1 and 2 present the 2D plate at $t = 10ms$ and the 3D cube at $t = 7.5ms$. The not penetrated region at the center in the 2D plate has a square form, while it has a cylindrical form in the 3D case. Fig. 3 presents the partial penetration at $t = 11ms$ for the second 3D case. We observe similarities on iso-value distributions (Fig.2 and Fig.3). Note that the 3D case is similar to the 2D one when $\overrightarrow{\nabla} \cdot \overrightarrow{E} = 0$ without the demagnetizing field.

Full penetration: The penetration times are different. The full penetration is reached at $t = 19ms$ for the 2D plate, at $t = 12ms$ for the 3D cube. This discreapancy is dued to the demagnetizing field and $\overrightarrow{\nabla} \cdot \overrightarrow{E} \neq 0$. In the 2D case, all the iso-values go from the corners to the center (Fig.4), while they go from the top and bottom sides to the center in the 3D case (Fig.5). The penetration time of the second 3D case is $t = 13ms$ and similarities in both 3D distributions are observed (see Figs. 5 and 6). The iso-value distribution in the surrounding volume is presented in Fig.7.

Dissipated energy: Dissipated energy $W = \int_0^t \int_\Omega \overrightarrow{E} \cdot \overrightarrow{J} d\Omega dt$ is computed in different cases and compared to that obtained from a Finite Volume Method with $A-V$ formulation in Fig.8. In these published works, a surrounding volume is added and Dirichlet boundary conditions are used to impose the magnetic field without a time shift on the penetration [11]. A good agreement is observed between the results without a surrounding volume and the results obtained from an $A-V$ formulation. When the demagnetising effects are neglected in the $3D$ case, the total magnetic field is undervalued, penetration of current density is slower and the dissipated energy is less important in transient regime. Beyong $t = 15ms$, these energies are close and have linear evolutions as the applied magnetic field. There is a big gap between $2D$ and $3D$ energies that highlights necessity to develop $3D$ models

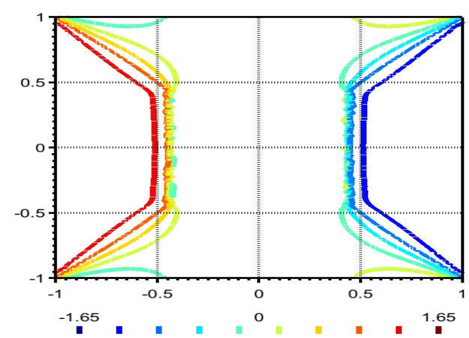

Fig. 1. Partial penetration: 2D iso-value distribution of J_y/J_c at $t = 10ms$

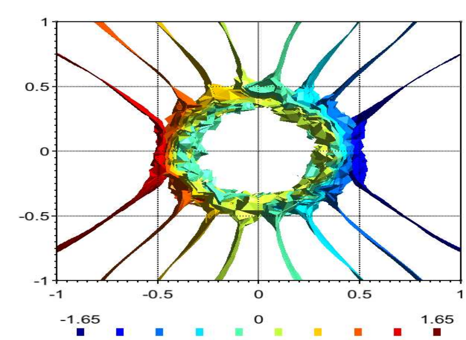

Fig. 2. Partial penetration: 3D iso-value distribution of J_y/J_c at $t = 7.5ms$

V. Conclusion

A semi implicit approach based on a nodal discontinuous Galerkin method is proposed to describe the current density in superconducting materials. The results have been compared with those obtained from a method using a surrounding vacuum volume.

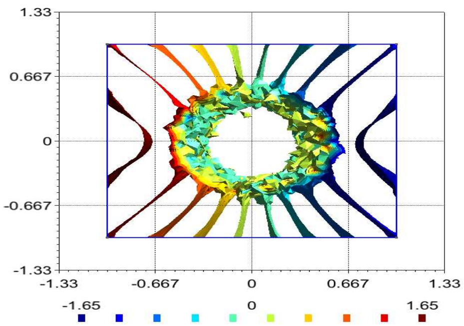

Fig. 3. Partial penetration: 3D iso-value distribution of J_y/J_c at $t = 11ms$ obtained with a surounding volume

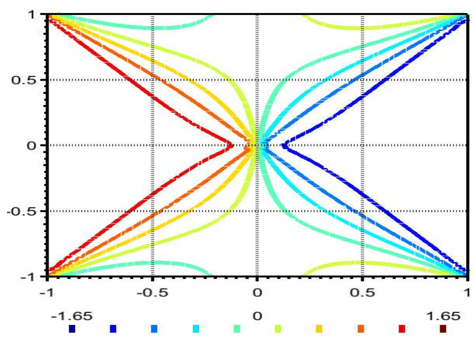

Fig. 4. Full penetration: 2D iso-value distribution of J_y/J_c at $t = 19ms$

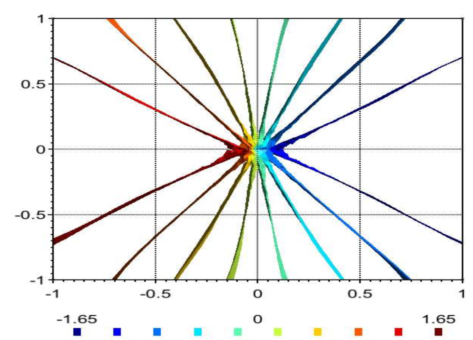

Fig. 5. Full penetration: 3D iso-value distribution of J_y/J_c at $t = 12ms$

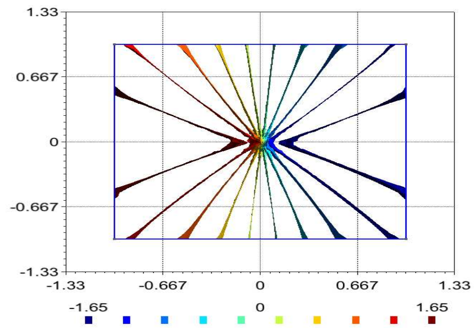

Fig. 6. Full penetration: 3D iso-value distribution of J_y/J_c at $t = 13ms$ obtained with a surounding volume

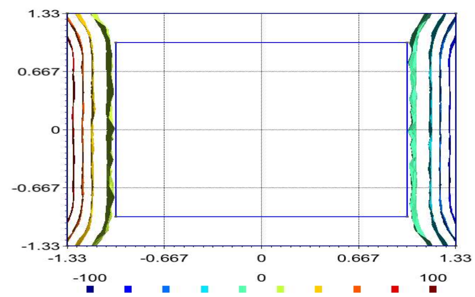

Fig. 7. 3D iso-value distribution of J_y/J_c inside the surounding conductor when the full penetration of superconducting cube is reached

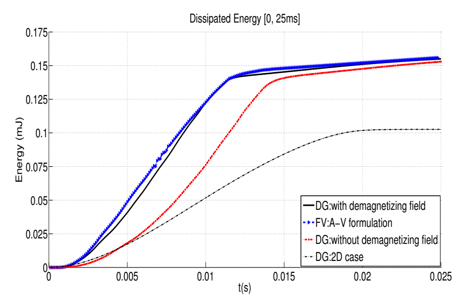

Fig. 8. Comparison of the dissipated energy during $[0, 25ms]$

REFERENCES

[1] A. Bossavit *Numerical modeling of superconductors in three dimensions: A model and a finite element method.* IEEE Trans. Magn., Vol. 30, number 5, p3363-3366, 1994.

[2] E. Zeldov and al *Flux creep characteristics in high temperature superconductors.* Appl. Phy. Let., Vol. 56, number 7, p680-683, 1990

[3] G. Meunier, P. Tixador *Differents formulation to models superconductors.* IEEE Trans. Magn., Vol. 36, number 4, p3445-3448, 2000.

[4] A. Kameni and al *A 2D robust FE-FV mixed method to handle strong nonlinearities in superconductors.* IEEE Trans. Magn., Vol. 46, number 8, p3445-3448, 2010.

[5] Z. Hong, A. M. Campbell, T. A. Coombs *Computer Modeling of Magnetisation in High Temperature Bulk Superconductors* IEEE Trans. Magn., Vol. 17, number 2, p3761-3764, 2007.

[6] F. Grilli and al *Finite-element method modeling of superconductors: from 2-D to 3-D* IEEE Trans. Appl. Supercond., Vol. 15, number 1, p17-25, 2004.

[7] M. Zhang and T.A. Coombs *3D modeling of high-Tc superconductors by finite element software.* Supercond. Sci. Tech., Vol.25, number1, p15009-15016, 2012

[8] D. N. Arnold, F. Brezzi, B. Cockburn and L.D. Marini *Unified analysis of discontinuous galerkin methods for elliptic problems*, SIAM J. Numer. Anal, Vol 39, number 5, p1749-1779, 2002.

[9] A. Kameni and al *Discontinuous Galerkin Methods for computing induced fields in superconductors* IEEE Trans. Magn., Vol. 48, number 2, p3445-3448, 2012.

[10] H.W. Alt and S. Luckhaus *Quasilinear elliptic-parabolic differential equations* Math. Zeit., Vol. 83, number 6, p311-341, 1983.

[11] L. Allaoui and F. Bouillault *Numerical study of the influence of flux creep and of thermal effect on dynamic behaviour of magnetic levitation systems with a high-Tc superconductor using control volume method* Eur Phys J Applied Phys, Vol. 25, number 1, 2012.

[12] A. Aharoni *Demagnetizing factor for rectangular ferromagnetic prisms* J. Appl. Phys., Vol. 83, number 6, 1998.